Scott, R. A. (1985) *Methods Enzymol. 117*, 414–459.
Scott, R. A., & Dooley, D. M. (1985) *J. Am. Chem. Soc. 107*, 4348–4350.
Scott, R. A., Cramer, S. P., Shaw, R. W., Beinert, H., & Gray, H. B. (1981) *Proc. Natl. Acad. Sci. U.S.A. 78*, 664–667.
Scott, R. A., Schwartz, J. R., & Cramer, S. P. (1984) in *EXAFS and Near Edge Structure III* (Hodgson, K. O., Hedman, B., & Penner-Hahn, J. E., Eds.) pp 111–116, Springer-Verlag, Berlin.
Scott, R. A., Schwartz, J. R., & Cramer, S. P. (1986) in *Biological and Inorganic Copper Chemistry* (Karlin, K. D., & Zubieta, J., Eds.) Vol. I, pp 41–52, Adenine Press, New York.
Sugiura, Y., Hirayama, Y., Tanaka, H., & Ishizo, K. (1975) *J. Am. Chem. Soc. 97*, 5577–5581.
Teo, B.-K., & Lee, P. A. (1979) *J. Am. Chem. Soc. 101*, 2815–2832.
Wikström, M., Krab, K., & Saraste, M. (1981) in *Cytochrome Oxidase. A Synthesis*, Academic Press, New York.
Yonetani, T. (1961) *J. Biol. Chem. 236*, 1680–1688.

Environmental Modulation of C-Terminus Dynamic Structure in Bacteriorhodopsin†

Jeffrey Marque,*,‡ Kazuhiko Kinosita, Jr.,‡ Rajni Govindjee,§ Akira Ikegami,‡ T. G. Ebrey,§ and Jun Otomo‡
Institute of Physical and Chemical Research, Hirosawa, Wako-shi, Saitama 351-01, Japan, and Department of Physiology and Biophysics, University of Illinois at Urbana-Champaign, Urbana, Illinois 61801
Received December 12, 1985; Revised Manuscript Received April 7, 1986

ABSTRACT: We used steady-state and time-resolved (pulsed) fluorescence spectroscopies to study the dynamic structure of the COOH terminus in bacteriorhodopsin. The extrinsic fluorophore 8-aminonaphthalene-1,3,6-trisulfonic acid was attached to the protein, in purple membrane sheets, with a water-soluble carbodiimide; about 50% of the dye molecules were found to be attached to the COOH terminus. Signals from samples treated with papain were subtracted from non-papain-treated sample signals to give information about the COOH-terminus dynamics. Dye molecules on the COOH terminus fluoresce more strongly than dye molecules bound elsewhere on the membrane. This result, combined with our calculations showing that retinal is an energy acceptor in our system, suggests that the C-terminus spends most of its time away from the membrane surface. We systematically studied the effects of temperature, ionic strength, and pH, fitting the time-resolved anisotropy to $r(t) = r_\infty + (r_0 - r_\infty)e^{-t/\phi}$; the following picture emerged: In the pH range 5.6–10.9, raising the pH has the effect of increasing the fluorescence intensity and decreasing r_∞. We interpret this result to mean that the time-averaged position of the COOH terminus becomes farther from retinal as the pH is raised and that the range of Brownian motions of the C-terminus increases along with the pH. At pH 6.6, adding NaCl up to a concentration of 10 mM had qualitatively the same effects as raising the pH. Over the temperature range 10–50 °C, the time constant for anisotropy decay scales closely with the viscosity of water, a result consistent with Brownian motions of the COOH terminus in bulk water. We invariably found that $r_0 > 2r_\infty$. All of our results are consistent with the conclusion of Wallace and Henderson [Wallace, B. A., & Henderson, R. (1982) *Biophys. J. 39*, 233] that the COOH terminus of bacteriorhodopsin is free to assume many positions.

Bacteriorhodopsin (bR) is the sole protein constituent of purple membrane (PM), the light-driven proton pump that is part of the cell membrane in some strains of *Halobacterium halobium*. Bacteriorhodopsin is a single polypeptide containing seven α-helices that span the membrane; the final 20–25 amino acid residues at the carboxy terminus can be cleaved by papain digestion. These facts, plus further details on the structure and function of bR and PM, are covered in several review articles (Stoeckenius et al., 1979; Stoeckenius & Bogomolni, 1982; Dencher, 1983).

We have studied the dynamic structure of the carboxy terminus via steady-state and time-resolved fluorescence depolarization spectroscopy techniques. We are particularly interested in the pH and ionic strength dependence of the dynamic structure because pH and salt concentration are known to affect the kinetics of the proton pump and photocycle (Ort & Parson, 1978; Li et al., 1984; Govindjee et al., 1980). Although this is hardly surprising behavior in a proton pump, the mechanism of the effect is not yet established. A priori, the pH effect could simply be a concentration (of protons) effect, but we shall show in this paper that both the freedom of motion of the C-terminus and its distance from the membrane surface are, under some conditions, affected by the pH and ionic strength of the suspending medium.

Renthal et al. (1983) published the first fluorescence study of the bR C-terminus mobility. They attached the fluorophore danzylhydrazine to PM with a water-soluble carbodiimide, and they found that most of the probe was attached to the C-terminus. At a pH of 8.0 [0.05 M tris(hydroxymethyl)-aminomethane (Tris)], they found that the steady-state po-

† This research was supported by Grants NSF INT 8313642 and NSF INT 8213638 from the National Science Foundation (U.S.–Japan Program in Photoconversion and Photosynthesis), by a research grant for solar energy conversion–photosynthesis from the Agency of Science and Technology of Japan, and by special coordination funds for the promotion of science and technology from the Agency of Science and Technology of Japan.
* Address correspondence to this author at the School of Applied and Engineering Physics, Cornell University, Ithaca, NY 14853.
‡ Institute of Physical and Chemical Research.
§ University of Illinois at Urbana–Champaign.

0006-2960/86/0425-5555$01.50/0

larization of fluorescence was 0.24, and they interpreted this as indicating restricted motion of the fluorophore. We decided to perform a variation on the above work with two important differences. First, we used a more hydrophilic probe to minimize probe–lipid attractions. Second, we systematically studied the pH, ionic strength, and temperature dependence of the mobility of the probe attached to the C-terminus.

Materials and Methods

Purple Membrane Isolation and Purification. Purple membranes were prepared from *Halobacterium halobium*, strain ET1001, according to an established procedure (Oesterhelt & Stoeckenius, 1974) but with sonication for final purification (Braiman & Mathies, 1980). Purity of the membranes was checked by sodium dodecyl sulfate (SDS) gel electrophoresis. All PM used for fluoresence spectroscopy showed a single band on the gel prior to modifications (e.g., fluorophore attachment).

Attachment of Fluorophore to Protein. The procedure that we used to label the protein with an extrinsic fluorophore is a modification of the procedure developed by Renthal et al. (1983). A stock solution of the fluorophore 8-aminonaphthalene-1,3,6-trisulfonic acid disodium salt (Molecular Probes, Inc., Junction City, OR), hereafter referred to as ANTSA, was adjusted to pH 5. A fresh aqueous solution of *N*-[3-(dimethylamino)propyl]-*N'*-ethylcarbodiimide hydrochloride (Merck-Schuchardt, West Germany), hereafter referred to as EDC, was adjusted to pH 5. The fluorophore–protein coupling reaction was started by combining solutions of reactants with the following concentrations: bacteriorhodopsin (in purple membrane), 50 μM; ANTSA, 25 mM; EDC, 2 mM; NaCl, 0.5 M. The reaction was allowed to proceed with stirring for 2 h at room temperature in the dark. The pH was monitored continuously and kept within 0.1 pH unit of pH 5.0. The reaction suspension was centrifuged at 100000*g* for 30 min at 5 °C, the pellet resuspended in 10 mL of ice–water, and the sample centrifuged again as before. The resuspension and centrifugation procedure was repeated 8 more times, at which point no free ANTSA could be detected in the suspension. (The method for discriminating between free and bound dye is described later.)

Estimation of Dye/Protein Stoichiometry. The average number of dye molecules bound to each bR molecule was determined by (1) measuring the absorbance of an ANTSA–PM sample at 568 nm in order to determine the bR concentration, (2) measuring the fluorescence intensity from the same ANTSA–PM sample after denaturation of the bR and destruction of retinal, and (3) comparison of the data from (2) with the fluoresence intensity from a calibration solution in which the concentration of bound ANTSA was known. The details of the measurement are as follows:

(1) The shapes of the visible absorption spectra of the light-adapted forms of PM and ANTSA–PM (spectra not shown) are so similar that we assumed that the extinction coefficients are equal at 568 nm. The measurement of the bR concentration in ANTSA–PM thus proceeds in the same way as for ordinary PM (Stoeckenius et al., 1979). (2) As we shall show later, energy transfer can occur in ANTSA–PM between the fluorophore (donor) and retinal (acceptor). To estimate the concentration of bound ANTSA in ANTSA–PM via a fluorescence intensity measurement, it was therefore necessary to remove the acceptor. We did this by taking 2.85 mL of the suspension used in (1), adding 0.15 mL of 10% SDS, and irradiating with a mercury lamp until the yellow color (due to retinal) disappeared. The fluorescence intensity was then measured (excitation 310 nm; emission 420 nm). (3) The calibration solution for measurement 2 was made by adding 96 mg of EDC to 4.8 mL of 0.5 M acetate (pH 4.75), 0.175 mL of water, and 0.025 mL of 5 mM aqueous ANTSA. The acetate was in large excess compared with the ANTSA, and we can therefore be sure that the dye was bound quantitatively to acetate, giving a final concentration of 25 μM for the bound ANTSA.

To check whether or not the UV radiation in (2) also destroyed the bound ANTSA, we diluted the above calibration solution to 5 μM, added SDS to 0.5%, and irradiated with the mercury lamp for 3 h. The result was that there was no change in the fluorescence intensity or spectrum, suggesting that the ANTSA in our ANTSA–PM samples was not affected by the UV treatment.

Papain Treatment. We removed the C-terminus from ANTSA–PM by digesting the latter with papain, essentially as per the procedure described by Renthal et al. (1979). First, an activation solution of 0.05 M cysteine and 0.02 M ethylenediaminetetraacetic acid (EDTA), and a solution of ANTSA–PM (65 μM bR) were buffered to pH 8 with 0.05 M Tris. Digestion was initiated by adding 1 mL of the buffered ANTSA–PM to 0.2 mL of the activation solution and 0.12 mL of an aqueous papain solution (0.05 mg of papain/mL water). The reaction mixture was incubated at 37 °C for 4 h, with continuous mixing, and then cooled rapidly in ice–water. Washing and centrifugation were performed 5 times as described earlier. Effectiveness of papain digestion was always confirmed by SDS gel electrophoresis.

Steady-State Fluorescence Measurements. Samples that were used to study pH effects were suspended at an ANTSA–PM concentration of 2 μM bR. We used 0.5 mM buffers (pH 6 and 7, phosphate; pH 8 and 9, borate; pH 10 and 11, bicarbonate) (*Handbook of Biochemistry and Molecular Biology*, 1976). The suspension pH values were adjusted with dilute HCl or NaOH as necessary. For measurement of the effects of ionic strength on the dynamic structure, samples were suspended in 100 μM sodium phosphate buffer (pH 6.6) at an ANTSA–PM concentration of 4 μM bR. Ionic strength was varied by adding aliquots of NaCl solutions. For all fluorescence spectroscopy, the sample was contained in a quartz cuvette fitted with a ground-glass joint cap to retard the diffusion of atmospheric CO_2 into the samples. Fluorescence intensities and corrected spectra were measured in a Hitachi 650-60 fluorescence spectrophotometer that included removable excitation and emission polarizers for anisotropy measurements. We took the following precautions in order to decrease artifactual errors in our steady-state data: Two sharp-cut filters (SC-37, Fuji Film, Tokyo) were placed between the sample and the emission monochromator to reduce the scattered light detected at the photomultiplier. Also, a UV 330 filter (Hoya, Tokyo) was placed between the sample and the excitation monochromator to prevent long-wavelength light from entering the sample chamber.

Time-Resolved Fluorescence Spectroscopy. Our measurements were performed on an instrument described in papers where the method of deconvoluting and fitting the data is also described (Kawato et al., 1977; Kinosita et al., 1981). The excitation monochromator was set to 310 nm ($\Delta\lambda \simeq 8$ nm), and two excitation filters were used to enhance monochromaticity (UV-D33S filter, Toshiba, Tokyo). The samples were prepared in the same way as for steady-state measurements. Temperature control, via water circulation through the cuvette-holding block, was always better than 0.1 °C. No emission monochromators were used. Two SC-37 filters and one SC-38 filter, placed between the sample and each of the

two photomultiplier tubes, allowed us to collect most of the fluorescence with wavelength longer than 380 nm.

In this paper we make qualitative interpretations of the time-resolved data on the basis of concepts from a wobbling-in-cone model (Kinosita et al., 1977). The model involves fitting the anisotropy decay data to a single exponential function:

$$r(t) = (r_0 - r_\infty) \exp(-t/\phi) + r_\infty \quad (1)$$

The cone angle and the wobbling-in-cone diffusion constant are then calculated from the three-fit parameters r_0, r_∞, and ϕ. The cone angle θ_c is a function of only two of the fit parameters:

$$\frac{r_\infty}{r_0} = \left[\frac{\cos\theta_c}{2}(1 + \cos\theta_c)\right]^2 \quad (2)$$

The wobbling-in-cone diffusion constant is a function of all three parameters. However, in a comparison of all of our data sets, the spread in $r_0 - r_\infty$ is sufficiently small so that changes in the wobbling-in-cone diffusion constant are essentially reflected in the changes of ϕ only.

The interpretation of $r(t)$ for our data is complicated by the fact that the intensity decay is not monoexponential for ANTSA–PM (see Figure 2). However, we shall present evidence that suggests that the C-terminus is in the bulk aqueous phase. The rotation of the various (heterogeneous-bound) fluorophores on the terminus is hence probably similar, so that qualitative interpretations of diffusion constants and amplitudes of rotation, particularly with regard to their functional dependence on pH, temperature, and ionic strength, are valid.

We measured the limiting anisotropy (r_0) of ANTSA–acetate by measuring the steady-state and time-resolved anisotropies in 100% glycerol at 0 °C. The time-resolved measurement gave a limiting anisotropy of 0.252, with a very slow decay (266 ns). The steady-state value agreed within 4%. For all of the fit parameters given in this paper, the constraint of $r_0 = 0.252$ was imposed on the fitting algorithm.

Results and Discussion

We first present a summary of the essential features of our data and of our interpretations. (1) Increasing the pH of the ANTSA–PM suspension had the effect of increasing the steady-state fluorescence intensity, decreasing the rate of the (time-resolved) fluorescence decay, and decreasing r_∞. We interpret these results to mean that at higher pH the average position of the C-terminus is farther away from retinal and that the angular extent of its Brownian motions is larger. (2) At higher temperatures the fluorescence intensity decreases, and the rate of decay in the fluorescence anisotropy increases. The time constant of the anisotropy decay scales approximately with the viscosity of water. We interpret the data to mean that the C-terminus is probably surrounded by bulk (as distinct from bound) water and that temperature variations do not significantly affect the angular limits of Brownian motions of the C-terminus. (3) Increasing the ionic strength of the suspension with sodium chloride had effects that were qualitatively the same as the effects of raising the pH; that is, the fluorescence intensity increased, the rate of the fluorescence decay decreased, and r_∞ decreased.

Details of Results and Discussion. The fluorescence spectrum of ANTSA changes dramatically when it is bound to purple membrane or acetic acid (Figure 1). The fluorescence of the free dye at 420 nm, when excited at 310 nm, is less than 2% that of the bound dye. Hence, two properties of the dye made it very convenient for these measurements: (1) its hydrophilicity made it easy to wash out the excess free dye after binding to the membrane; (2) the large shift in the fluorescence spectrum after binding made it possible to do bound-dye spectroscopy with very little signal from what little (undetectable) free dye may have remained in the ANTSA–PM.

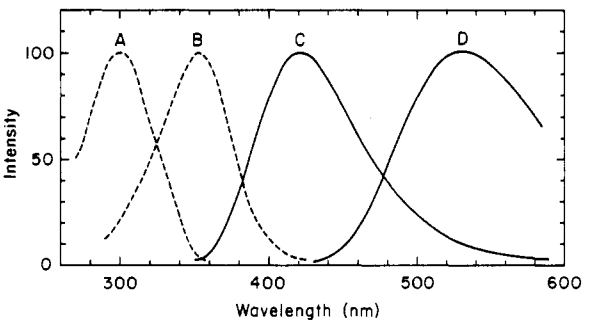

FIGURE 1: Excitation and emission spectra of free aqueous ANTSA and ANTSA bound to bR or acetate. Intensity shown is relative. ANTSA concentration is 2 μM in water. (A) Bound, excitation with λ_{em} = 420 nm; (B) free, excitation with λ_{em} = 530 nm; (C) bound, emission with λ_{ex} = 310 nm; (D) free, emission with λ_{ex} = 355 nm.

We found that, in the absence of an energy acceptor, the molecular environment around bound ANTSA had only small effects on the fluorescence intensity and lifetime. For example, the fluorescence intensities from ANTSA-bleached PM (bleaching via hydroxylamine plus light, prior to labeling) vs. ANTSA-bleached PM in 0.5% SDS differed by only 30%. The fluorescence intensity decay time constants for ANTSA–acetate in 100%, 90%, and 50% glycerol and in 100% water were 7.6, 7.2, 6.5, and 6.5 ns, respectively, all at 20 °C, and for ANTSA-bleached PM (via hydroxylamine) and ANTSA–PM in 0.5% SDS (after UV irradiation) were 6.0 and 5.8 ns, respectively. The excitation spectra (λ_{em} = 420 nm) and emission spectra (λ_{ex} = 310 nm) for ANTSA–acetate in various aqueous solutions of ethanol and 2-propanol (varying from 100% water to 100% alcohol) show only a 15% spread in the peak heights and 10-nm total spread in the peak locations. The emission peak location is insensitive to pH. We found that the fluorescence intensity of ANTSA–acetate was insensitive to the addition of NaCl in the range of ionic strengths that we studied (≤10 mM). All of these control data, taken together, show that the fluorescence changes are small even when the microenvironment around bound ANTSA is drastically changed with SDS, glycerol, alcohols, and so forth. These control data, together with the fact that the spectra for ANTSA–bR and ANTSA–acetate are indistinguishable, support the reliability of our dye/protein stoichiometry measurements since they indicate that the calibration sample is directly comparable to the bleached sample.

Förster's (1965) theory was used to calculate the critical energy-transfer distance between the bound dye and retinal. The overlap integral was measured to be $(7.0 \pm 0.6) \times 10^{-14}$ M^{-1} cm^3, the quantum yield was 0.27, the refractive index was assumed to be 1.41, and the orientation factor was taken to be $^2/_3$. (The latter assumes random relative orientation of acceptor and donor.) This yields a critical distance of 3.7–3.8 nm. The fluorescence decay times for all of our ANTSA–PM samples were in the range 2–3 ns, or about half the value found when an energy acceptor was absent. This suggests that 3.7 nm, the critical distance, is typical for the average distance between the fluorophore and retinal. We thus expect that, in our ANTSA–PM samples, the fluorescence lifetime is sensitive to changes in the retinal–dye distance because the dependence of the lifetime on distance is steepest when the distance is the critical distance. Furthermore, this calculated critical distance

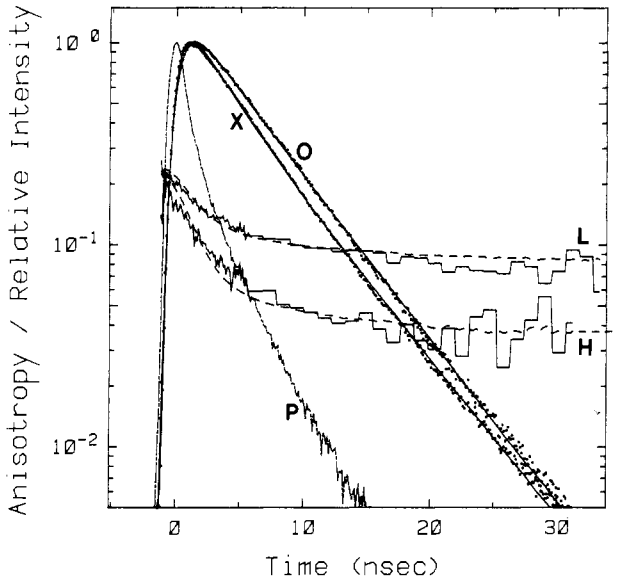

FIGURE 2: Time-resolved fluorescence intensity (normalized) for ANTSA–PM suspensions at pH 5.6 (X) and pH 9.5 (O), along with their respective time-resolved anisotropies (L and H). All fit parameters given in this paper were obtained after deconvolution of the intensity data from the light-pulse profile (P) and therefore correspond to the response to a δ-function light pulse. The dashed line is the best fit to eq 1. Solid lines for the intensity data are the best fits to two-exponential decay functions. The temperature was 20.0 °C.

suggests that the fluorophores are in the aqueous phase: there is probably no location in or on the membrane that is 37 Å away from all retinal moieties.

There was some variability in the stoichiometry of binding. Before papain treatment, the dye/protein ratio in our ANTSA–PM samples ranged from about 1.6 to 2.0, as determined by the calibration procedure described earlier. After the ANTSA–PM samples were treated with papain, the ratio fell to about 0.6–1.0, so roughly half of the fluorophores coupled to the C-terminus. However, the ratio of fluorescence intensities from ANTSA–PM vs. papain-treated ANTSA–PM was always about 3. These results are consistent with our measurements and calculations (the results of which were briefly described above), which show that retinal acts as an energy acceptor in ANTSA–PM, and with the interpretation that dye molecules bound to the C-terminus are farther away from retinal than dye molecules that are bound elsewhere to the purple membrane. In other words, the fluorophores on the C-terminus give a disproportionately high contribution to the fluorescence intensity (compared with fluorophores bound elsewhere) because they are, on the average, farther away from retinal.

Except where specifically noted otherwise, all of the spectroscopic results presented below were obtained by subtracting the papain-treated ANTSA–PM signal from the ANTSA–PM signal so as to obtain the signal coming only from the C-terminus.

Figure 2 shows typical data sets that were collected when we studied pH effects in the time-resolved spectrofluorometer. The increase in r_∞, as the pH is decreased, is clear. Figure 3 shows the pH dependence of r_∞. Over the range 10.9–5.6, the value of r_∞ increases by a factor of 3 for fluorophores on the terminus. However, even the highest value that we measured for r_∞, 0.11, when compared with our measured limiting anisotropy of 0.252, suggests a very freely moving C-terminus. Our data are in marked contrast to the data of Renthal et al. (1983). Their data are consistent with their interpretation that the C-terminus Brownian motions are

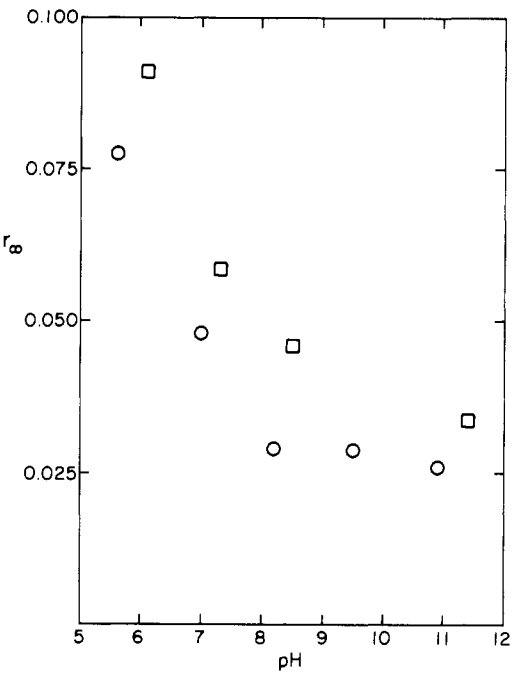

FIGURE 3: pH dependence of r_∞ for ANTSA–PM suspensions at 20.0 °C. The data shown are for samples for which papain-treated blanks were (circles) and were not (squares) used. These data show an invariant feature of all of our data sets: The omission of use of a papain-treated blank gave higher anisotropy values. The C-terminus, whose dynamics were studied by using papain-treated blanks, always showed lower r_∞ (and steady-state anisotropies) than ANTSA–PM samples under otherwise identical conditions.

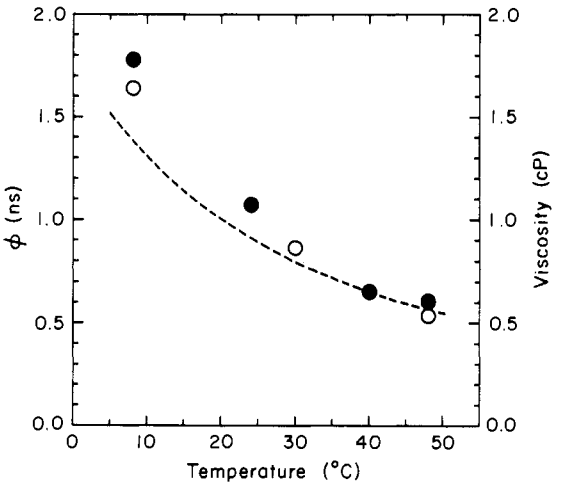

FIGURE 4: Temperature dependence of anisotropy decay time constant for ANTSA–PM suspensions at pH 10.4 (O) and pH 5.6 (●), shown together with the viscosity of water (dashed line). The values for ϕ were found by fitting the time-resolved anisotropy data to eq 1 along with the fitting constraint $r_0 = 0.252$.

highly constrained. We do not know the reasons for the discrepancy between their and our data, but the difference in the hydrophobicity of danzylhydrazine as compared with ANTSA may be a critical factor.

As the NaCl concentration was increased from 0 to 10 mM, the steady-state anisotropy smoothly decreased from 0.17 to 0.13, and the fluorescence intensity smoothly and monotonically increased by 10% (Govindjee et al., 1984). Furthermore, for measurements of the steady-state intensity in which no papain-treated blank was used, the intensity increased by about 5% as the pH increased from 6 to 11. Over the same range, the steady-state anisotropy monotonically decreased from 0.18 to 0.11.

Consider now the temperature dependence of the characteristic decay time for the anisotropy. Figure 4 shows the data together with a superimposed plot of the viscosity of water over the same temperature range. Although the scaling is not exact, it suggests that the C-terminus is in the aqueous phase. In these same time-resolved measurements, r_∞ does not vary with temperature within the errors of our fit parameters. In the temperature range we studied (10–50 °C), there are apparently no changes in the angular limits of the Brownian motions of the C-terminus, suggesting that there are no changes in protein or lipid structure that alter the strength of interaction between C-terminus and membrane.

The time-resolved measurements also suggest that the main effect of pH is not on the structure of the C-terminus. For example, the average anisotropy decay time decreases from about 1.5 ns at pH 6 to 1.1 ns at pH 11 (data not shown), a change of less than 40%. This compares with a change by a factor of 3 for r_∞ over the same pH range and suggests that neither the local viscosity nor the C-terminus structure varies greatly with pH.

The facts that the r_∞ values in all of our time-resolved measurements are small (less than 0.11) compared with the limiting anisotropy (0.252), that the time constant of the average anisotropy decay scales closely with the viscosity of water, and that the intensity of fluorescence from dye molecules on the C-terminus is greater than the intensity from dye molecules on or under the membrane surface are all consistent with the C-terminus being located, most of the time, in the aqueous phase. Our data suggest a picture of the C-terminus as moving randomly in the aqueous phase except for the constraint imposed by its attachment at the membrane surface. Our data and interpretations are also consistent with a main conclusion from work of Wallace and Henderson (1982) that the C-terminus is free to take up many positions.

The functional dependences that we have described above (for example, the decrease in r_∞ as the pH is raised) occurred invariably, that is, for every sample for which a measurement was made. There was variability of about 10% when comparing specific parameter fits from different ANTSA–PM batches, but there was no variability in the data trends. We therefore have confidence in our interpretations because they were derived primarily from the functional behavior of the fit parameters.

Do our time-resolved data reflect motions of the C-terminus or only of the bound dye? The following measurement suggests that C-terminus motions must be involved: A time-resolved measurement for ANTSA–acetate in 90% w/w glycerol at 20 °C (that is, about 220 cP) gave an anisotropy decay constant of 27 ns. The corresponding time constant in water at the same temperature (1 cP) is calculated to be 0.12 ns, faster than we can measure and more than an order of magnitude faster than the fastest average anisotropy decay that we observed in the C-terminus. We conclude that C-terminus motions contribute predominantly to the anisotropy decays that we have reported here.

The apparent increase in the retinal–dye distance that we observed when we increased the ionic strength of the suspension up to 10 mM is opposite to what one might have expected: Coulombic repulsion between the negatively charged membrane surface and the negatively charged residues (and fluorophores) on the C-terminus would be expected to maximize that distance. The screening from added salt would be expected to decrease the distance. An idea that is consistent with our data, and which attempts to resolve the above paradox, is as follows: A cluster of positively charged residues on the C-terminus side of the membrane attracts the C-terminus when the ionic strength and pH are low. Increasing the pH decreases the time-averaged positive charge on these residues; increasing the ionic strength screens the attraction. Good candidates for the residues in the cluster are Lys-172, Arg-175, Arg-225, Arg-227, and Arg-164 (Agard & Stroud, 1982; Trewhella et al., 1983). In thinking about this idea, and about the data that we present in this paper, it should be borne in mind that we report here on fluorescence properties of modified, not native, membranes. The highly charged dye may experience stronger interactions than occur between carboxylate residues and surrounding charges in the native membrane.

ACKNOWLEDGMENTS

We thank H. J. Weber for the *H. halobium* strain ET1001 that was used in this study. We also express thanks to Dr. T. Kouyama for his many helpful suggestions, for his technical assistance with the measurements, and for his discussions about this study. We thank Anne Kingsley from the School of Applied and Engineering Physics at Cornell University for editorial assistance.

Registry No. Retinal, 116-31-4.

REFERENCES

Agard, D. A., & Stroud, R. M. (1982) *Biophys. J. 37*, 589.
Braiman, M., & Mathies, R. (1980) *Biochemistry 19*, 5421.
Dencher, N. A. (1983) *Photochem. Photobiol. 38*(6), 753.
Förster, Th. (1965) in *Modern Quantum Chemistry* (Sinanoglu, O, Ed.) Part III, pp 93–137, Academic, New York.
Govindjee, R., Ebrey, T. G., & Crofts, A. R. (1980) *Biophys. J. 30*, 231.
Govindjee, R., Kinosita, K., Ikegami, A., & Ebrey, T. (1984) *Biophys. J. 45*, 214a.
Handbook of Biochemistry and Molecular Biology (1976) Vol. I, 3rd ed., pp 358–359, CRC Press, Boca Raton, FL.
Kawato, S., Kinosita, K., Jr., & Ikegami, A. (1977) *Biochemistry 16*, 2319.
Kimura, Y., Ikegami, A., Ohno, K., Saigo, S., & Takeuchi, Y. (1981) *Photochem. Photobiol. 33*, 435.
Kinosita, K., Jr., Kawato, S., & Ikegami, A. (1977) *Biophys. J. 20*, 289.
Kinosita, K., Jr., Kataoka, R., Kimura, Y., Gotoh, O., & Ikegami, A. (1981) *Biochemistry 20*, 4270.
Li, Q., Govindjee, R., & Ebrey, T. G. (1984) *Proc. Natl. Acad. Sci. U.S.A. 81*, 7079.
Oesterhelt, D., & Stoeckenius, W. (1974) *Methods Enzymol. 31A*, 667.
Ort, D. R., & Parson, W. W. (1978) *J. Biol. Chem. 253*, 6158.
Renthal, R., Harris, G. J., & Parrish, R. (1979) *Biochim. Biophys. Acta 547*, 258.
Renthal, R., Dawson, N., Tuley, J., & Horowitz, P. (1983) *Biochemistry 22*, 5.
Stoeckenius, W., & Bogomolni, R. A. (1982) *Annu. Rev. Biochem. 52*, 587.
Stoeckenius, W., Lozier, R. H., & Bogomolni, R. A. (1979) *Biochim. Biophys. Acta 505*, 215.
Trewhella, J., Anderson, S., Fox, R., Gogol, E., Khan, S., Engelman, D., & Zaccai, G. (1983) *Biophys. J. 42*, 233.
Wallace, B. A., & Henderson, R. (1982) *Biophys. J. 39*, 233.
Wallace, B. A., & Kohl, N. (1984) *Biochim. Biophys. Acta 777*, 93.